

**Identification and simulation of space-time variability of past
hydrological drought events in the Limpopo river basin, Southern
Africa**

**P. Trambauer ¹, S. Maskey ¹, M. Werner ^{1,2}, F. Pappenberger ³, L.P.H. van Beek ⁴,
S. Uhlenbrook ^{1,5}**

[1] UNESCO-IHE, Department of Water Science and Engineering, P.O. Box 3015, 2601 DA Delft,
The Netherlands

[2] Deltares, P.O. Box 177, 2600MH Delft, The Netherlands

[3] ECMWF, Shinfield Park, RG2 9AX Reading, United Kingdom

[4] Utrecht University, Dept. Physical Geography, Utrecht, The Netherlands

[5] Delft University of Technology, Water Resources Section, P.O. Box 5048, 2600 GA Delft, The
Netherlands

Correspondence to: P. Trambauer (p.trambauer@unesco-ihe.org)

Abstract

Droughts are widespread natural hazards and in many regions their frequency seems to be increasing. A finer resolution version ($0.05^{\circ} \times 0.05^{\circ}$) of the continental scale hydrological model PCR-GLOBWB was set up for the Limpopo river basin, one of the most water stressed basins on the African continent. An irrigation module was included to account for large irrigated areas of the basin. The finer resolution model was used to analyse hydrological droughts in the Limpopo river basin in the period 1979-2010 with a view to identifying severe droughts that have occurred in the basin. Evaporation, soil moisture, groundwater storage and runoff estimates from the model were derived at a spatial resolution of 0.05° (approximately 5 km) on a daily time scale for the entire basin. PCR-GLOBWB was forced with daily precipitation and temperature obtained from the ERA-Interim global atmospheric reanalysis product from the European Centre for Medium-Range Weather Forecasts. Two agricultural drought indicators were computed: the Evapotranspiration Deficit Index (ETDI) and the Root Stress Anomaly Index (RSAI). Hydrological drought was characterised using the Standardized Runoff Index (SRI) and the Groundwater Resource Index (GRI), which make use of the streamflow and groundwater storage resulting from the model. Other more widely used meteorological drought indicators, such as the Standardized Precipitation Index (SPI) and the Standardized Precipitation Evaporation Index (SPEI) were also computed for different aggregation periods. Results show that a carefully set up process-based model that makes use of the best available input data can identify hydrological droughts even if the model is largely uncalibrated. The indicators considered are able to represent the most severe droughts in the basin and to some extent identify the spatial variability of droughts. Moreover, results show the importance of computing indicators that can be related to hydrological droughts, and how these add value to the identification of hydrological droughts/floods and the temporal evolution of events that would otherwise not have been apparent when considering only meteorological indicators. In some cases, meteorological indicators alone fail to capture the severity of the hydrological drought. Therefore, a combination of some of these indicators (e.g. SPEI-3, SRI-6, SPI-12 computed together) is found to be a useful measure for identifying from agricultural to long-term hydrological droughts in the Limpopo river basin. Additionally, it was possible to make a characterisation of the drought severity in the basin, indicated by its time of occurrence, duration and intensity.

Keywords: drought, hydrological model, Limpopo

1 Introduction

Droughts are a widespread natural hazard worldwide, and the societal impact is tremendous (Alston and Kent, 2004; Glantz, 1987). Recent studies show that the frequency and severity of droughts seems to be increasing in some areas as a result of climate variability and climate change (IPCC, 2007; Patz et al., 2005; Sheffield and Wood, 2008; Lehner et al., 2006). Moreover, and probably more importantly, the rapid increase of world population will certainly aggravate water shortage at local and regional scale. The study of droughts and drought management planning has received increasing attention in recent years as a consequence.

Drought monitoring is a key step in drought management, requiring appropriate indicators to be defined through which different types of drought can be identified. Meteorological, agricultural, and hydrological drought indicators are available to characterise different types of droughts. The most well known indicators are the Standardized Precipitation Index (SPI, McKee et al., 1993) and the Palmer Drought Severity Index (PDSI, Palmer, 1965; Dube and Sekhwela, 2007; Alley, 1984), both are primarily meteorological drought indices. SPI uses only precipitation in its computation, and PDSI uses precipitation, soil moisture and temperature. However, the timescale of drought that PDSI addresses is often not clear (Keyantash and Dracup, 2002), and will be usually determined by the time scale of the dataset; Vicente-Serrano et al. (2010b) indicate that monthly PDSI is generally correlated with SPEI at time scales of about 9-12 months. While the computation of PDSI is complex, applied to a fixed time window and difficult to interpret, SPI is easy to compute and to interpret in a probabilistic sense, is spatially invariant, and can be tailored to a time window appropriate to a user's interest (Guttman, 1998). Alley (1984) and Vicente-Serrano et al. (2010b) also highlight several limitations of PDSI, such as not allowing for the distinction of different types of drought (i.e., hydrological, meteorological, and agricultural) as it has a fixed temporal scale. The PDSI has other derivatives such as the Palmer Hydrological Drought Index (PHDI) for hydrological long-term droughts, Palmer Z Index for short term monthly agricultural droughts, and the CMI for short term weekly agricultural droughts. The empirical PDSI method developed in the United States, is still widely used in the United States but is gradually being substituted by other indicators in other regions (Keyantash and Dracup, 2002) as a result of its limitations. SPI can be computed for different time scales by accumulating the precipitation time series over the time period of interest (typically 3 months for SPI-3, 6 months for SPI-6, and 12 months for SPI-12). SPI has shown to be highly correlated with indicators of agricultural drought, hydrological drought, and groundwater drought. SPI-3 has a high temporal variability that is associated with short-to-medium range meteorological anomalies that can result in anomalous soil moisture and crop evolution, and can therefore be used as an indication of agricultural drought. SPI-6 has a higher correlation with hydrological droughts, mainly represented by low anomalies in runoff. SPI-12 and SPI-24 have a lower temporal variability and point to major and long duration drought events whose impacts may extend to groundwater. The widely used SPI does,

1 however, have its limitations mainly because it is based only on precipitation data. An extension of
2 SPI was proposed by Vicente-Serrano et al. (2010b) called the Standardized Precipitation Evaporation
3 Index (SPEI), which is based on precipitation and potential evaporation. In a way, it combines the
4 sensitivity of the PDSI to changes in evaporation demand with the capacity of SPI to represent
5 droughts on multi-temporal scale (Vicente-Serrano et al., 2010b).

6 Together with the development of the first drought indicators, hydrological models were also used for
7 agricultural and hydrological drought assessment. Schulze (1984) applied the ACRU hydrological
8 model in Natal, South Africa, to compare the severity of the 1979-1983 drought with other drought
9 events in the previous 50 years. He identified hydrological modelling as a potential powerful tool in
10 drought assessment and indicated that droughts in terms of water resources and crop yields do not
11 necessarily coincide.

12 In recent years, several new indicators have been developed to characterise the different types of
13 drought. Although drought indicators are mostly used to characterise past droughts and monitor
14 current droughts, forecasting of these indicators at different spatial and temporal scales is gaining
15 considerable attention.

16 In this study we extend a continental scale framework for drought forecasting in Africa that is
17 currently under development (Barbosa et al., 30 October to 1 November 2013), and apply this to the
18 Limpopo basin in southern Africa, one of the most water-stressed basins in Africa. The Limpopo river
19 basin is expected to face even more serious water scarcity issues in the future, limiting economic
20 development in the basin (Zhu and Ringler, 2012). To apply this framework at the regional scale, a
21 finer resolution version of the global hydrological model PCR-GLOBWB was adapted to regional
22 conditions in the basin. We model hydrological droughts and their space-time variability using a
23 process based distributed hydrological model in the (semi-) arid Limpopo basin. The model was tested
24 by comparing the simulated hydrological and agricultural drought indicators in the period 1979-2010
25 with reported historic droughts events in the same period. We derive a number of different drought
26 indicators from the model results (see Table 1), such as ETDI (Evapotranspiration deficit index,
27 Narasimhan and Srinivasan, 2005), RSAI (Root stress anomaly index), SRI (Standardized runoff-
28 discharge index, Shukla and Wood, 2008), and GRI (Groundwater resource index, Mendicino et al.,
29 2008). While the SRI is based on river discharge at a particular river section, the ETDI, RSAI and GRI
30 are spatial indicators that can be estimated for any location in the basin. ETDI and RSAI are directly
31 related to water availability for vegetation with or without irrigation, and GRI is related to
32 groundwater storage. Moreover, we compute the widely known meteorological drought indicators SPI
33 and SPEI at different aggregation periods to verify the correlation of the different aggregation periods
34 for these indices and the different types of droughts. Table 1 presents the derived indicators with a
35 description of the purpose and the type of drought each indicator represents. The aim of this study is to

1 assess the ability of different drought indicators to reconstruct the history of droughts in a highly water
2 stressed, semi-arid basin. Moreover, we investigate whether widely used meteorological indicators for
3 drought identification can be complemented with indicators that incorporate hydrological processes.

4 **2 Data**

5 **2.1 Study area: Limpopo river basin**

6 The Limpopo river basin has a drainage area of approximately 415,000 km² and is shared by four
7 countries: South Africa (45%), Botswana (20%), Mozambique (20%) and Zimbabwe (15%) (Fig. 1).
8 The climate in the basin ranges from tropical dry savannah and hot dry steppe to cool temperatures in
9 the mountainous regions. Although a large part of the basin is located in a semi-arid area, the upper
10 part of the basin is located in the Kalahari Desert where it is particularly arid. The aridity condition,
11 however, decreases further downstream. Rainfall in the basin is characterised as being seasonal and
12 unreliable causing frequent droughts, but floods can also occur in the rainy season. The average annual
13 rainfall in the basin is approximately 530 mm year⁻¹, which ranges from 200 to 1,200 mm year⁻¹ and
14 occurs mainly in the summer months (October to April) (LBPTC, 2010).

15 Arid and semi-arid regions are generally characterised by low and erratic rainfall, high inter-annual
16 rainfall variability and a low rainfall to potential evaporation ratio. This leads to the ratio of runoff to
17 rainfall being low at the annual scale. Hydrological modelling possesses considerable challenges in
18 such a region. A detailed discussion on problems related to rainfall-runoff modelling in arid and semi-
19 arid regions can be found in Pilgrim et al. (1988).

20 The runoff coefficient (RC = Runoff / Precipitation) of the Limpopo basin is remarkably low. For the
21 station at Chokwe (#24), which is the station with the largest drainage area among the discharge
22 stations available in this study (Fig. 1), the runoff coefficient is just 4.3% for the naturalised discharge
23 and a mere 1.7% for the observed discharge (without naturalisation). Note that the naturalised
24 discharge is estimated as observed discharge plus the estimated abstractions. These runoff coefficients
25 are strikingly low: out of 539 mm year⁻¹ of annual rainfall only 23 mm year⁻¹ (basin average) turns into
26 runoff annually including abstraction. This means that even a small error in estimates of precipitation
27 and evaporation could result in a large error in the runoff. Moreover, the uncertainty in the rainfall
28 input could easily be larger than the runoff coefficient (4.3%) of the basin. Runoff coefficients for
29 other selected stations in the basin (highlighted in Fig. 1, right panel) are presented in Table 2.

30 The basin is also highly modified as is evident from the observed and naturalised runoff. This adds an
31 additional challenge to model this basin. For example, for the largest drainage outlet available (#24),
32 the observed annual discharge is only some 39% of the naturalized discharge, which means that the
33 abstractions in the basin amount to 61% of the total runoff. Irrigation water demand takes up the
34 largest share. The total estimated present demand in the basin is about 4,700 x 10⁶m³yr⁻¹. The total

natural runoff generated from rainfall is approximately $7,200 \times 10^6 \text{m}^3 \text{yr}^{-1}$, showing that a significant portion of the runoff generated in the basin is currently used.

2.2 Data for the hydrological model

The Digital Elevation Model (DEM) we used is based on the Hydro1k Africa (USGS EROS, 2006). The majority of the parameters (maps) required for the model (e.g. soil layer depths, soil storage capacity, hydraulic conductivity, etc.) were derived mainly from three maps and their derived properties: the Digital Soil Map of the World (FAO, 2003), the distribution of vegetation types from GLCC (USGS EROS, 2002; Hagemann, 2002), and the lithological map of the world (Dürr et al., 2005). From the soil map, 73 different soil types were distinguished in the basin. The irrigated area was obtained from the global map of irrigated areas in 5 arc-minutes resolution based on Siebert et al. (2007) and FAO (1997). We computed the monthly irrigation intensities per grid cell using the irrigated area map, the irrigation water requirement data per riparian country in the basin and the irrigation cropping pattern zones (FAO, 1997).

All meteorological forcing data used (precipitation, daily temperature, daily minimum and maximum temperature at 2 meter) are the same as in Trambauer et al. (2014), and are based on the ERA-Interim (ERA-Interim) reanalysis dataset from the European Centre for Medium-Range Weather Forecasts (ECMWF). This dataset covers the period from January 1979 to present date with a horizontal resolution of approximately 0.7 degrees and 62 vertical levels. A comprehensive description of the ERA-Interim product is available in Dee et al. (2011). The ERA-Interim precipitation data used with the present model were corrected with GPCP v2.1 (product of the Global Precipitation Climatology Project) to reduce the bias with measured products (Balsamo et al., 2010). The GPCP v2.1 data are the monthly climatology provided globally at $2.5^\circ \times 2.5^\circ$ resolution, covering the period from 1979 to September 2009. The data set combines the precipitation information available from several sources (satellite data, rain gauge data, etc.) into a merged product (Huffman et al., 2009; Szczypta et al., 2011). From September 2009 to December 2010, the mean monthly ERA-Interim precipitation was corrected using a mean bias coefficient based on the climatology of the bias correction coefficients used for the period 1979-2009. While this only corrects for systematic biases, this was the only option available at the time, as a new version of GPCP (version 2.2) was not available. Temperature data is used for the computation of the reference potential evaporation needed to force the hydrological model. In this study the Hargreaves formula was used. This method uses only temperature data (minimum, maximum and average) so it requires less parameterization than Penman-Monteith, with the disadvantage that it is less sensitive to climatic input data, with a possibly reduction of dynamics and accuracy. However, it leads to a notably smaller sensitivity to error in climatic inputs (Hargreaves and Allen, 2003). Moreover, the potential evaporation derived from the Penman-Monteith equation and Hargreaves equation result in very similar values throughout Africa, and the choice of the method used

for the computation of the reference potential evaporation appears to have minor effects on the results of the actual evaporation for Southern Africa (Trambauer et al., 2014). For this study, the ERAI data were obtained for the period of 1979-2010. These were converted to the same spatial resolution as the model using bilinear interpolation to downscale from the ERAI grid to the 0.5° model grid. ERAI is archived using an irregular grid (reduced gaussian) over the domain and thus an interpolation was inevitable to be able to use it in the model.

Runoff data were obtained from the Global Runoff Data Centre (GRDC; <http://grdc.bafg.de/>), the Department of Water Affairs in the Republic of South Africa and ARA-Sul (Administração Regional de Águas, Mozambique). Runoff stations that have data available up until recent years, with relatively few missing data, are presented in Fig. 1. Most of these stations are in the South African part of the basin as almost no data could be found from stations in the other riparian countries. The sub-basins draining to each hydrometric station are named after the station number.

3 Methods

3.1 Process-based distributed hydrological model

3.1.1 General description

A processed based distributed hydrological (water balance) model based on PCR-GLOBWB (van Beek and Bierkens, 2009) is used. First the global scale model was adapted to the continent Africa (Trambauer et al., 2014). A higher resolution version (0.05° x 0.05°) of the continental model (0.5° x 0.5°) was applied for the Limpopo river basin. The PCR-GLOBWB was one of the 16 different land surface and hydrological models reviewed (Trambauer et al., 2013), and identified as one of the hydrological models that can potentially be used for hydrological drought studies in large river basins in Africa. PCR-GLOBWB is in many ways similar to other global hydrological models, but it has many improved features, such as improved schemes for sub-grid parameterization of surface runoff, interflow and baseflow, a kinematic wave based routing for the surface water flow, dynamic inundation of floodplains and a reservoir scheme (van Beek and Bierkens, 2009; van Beek, 2008).

On a cell-by-cell basis and at a daily time step, the model computes the water storage in two vertically stacked soil layers (max. depth 0.3 and 1.2 m respectively) and an underlying groundwater layer, as well as the water exchange between the layers and between the top layer and the atmosphere. It also calculates canopy interception and snow storage. Within a grid cell, the sub-grid variability is taken into account considering tall and short vegetation, open water and different soil types. Crop factors are specified on a monthly basis for short and tall vegetation fractions, as well as for the open water fraction within each cell. These crop factors are calculated as a function of the Leaf Area Index (LAI) as well as of the crop factors for bare soil and under full cover conditions (van Beek et al., 2011). Monthly climatology of LAI is estimated for each GLCC (Global Land Cover Characterization)-type,

using LAI values per type for dormancy and growing season from Hagemann et al. (1999). LAI is then used to compute the crop factor per vegetation type according to the FAO guidelines (Allen et al., 1998). The total specific runoff of a cell consists of the surface runoff (saturation excess), snowmelt runoff (after infiltration), interflow (from the second soil layer) and baseflow (from the lowest reservoir as groundwater). River discharge is calculated by accumulating and routing specific runoff along the drainage network and including dynamic storage effects and evaporative losses from lakes and wetlands (van Beek and Bierkens, 2009; van Beek, 2008). The default PCR-GLOBWB model does not explicitly consider irrigated areas but the version of the model used here includes an irrigation module to account for the highly modified hydrological processes in the irrigated areas of the basin.

3.2 Drought indicators

The meteorological drought indicators used in this study are computed only from meteorological variables: precipitation and potential evaporation. Agricultural and hydrological indicators, on the other hand, are computed from the results of the hydrological model, and therefore account for effects of soil, land use, groundwater characteristics, etc. in the basin. The indicators used in this study are described below.

3.2.1 Meteorological drought indicators

Standardised Precipitation Index (SPI)

The SPI was developed by McKee et al. (1993) and it interprets rainfall as a standardised departure with respect to a rainfall probability distribution. It requires fitting the precipitation time series to a gamma distribution function, which is then transformed to a normal distribution allowing the comparison between different locations. SPI [-] is then computed as the discrete precipitation anomaly of the transformed data divided by the standard deviation of the transformed data (Keyantash and Dracup, 2002; McKee et al., 1993). SPI values mainly range from 2.0 (extremely wet) to -2.0 (extremely dry).

Standardized Precipitation Evaporation Index (SPEI)

Instead of using only precipitation as in SPI, the SPEI uses the difference between precipitation (P) and potential evaporation (PET), i.e. $D = P - PET$, and the PET is computed following the Thornthwaite method (Vicente-Serrano et al., 2010a; Vicente-Serrano et al., 2010b). The calculated D values are aggregated at different time scales, following the same procedure as for the SPI. A log-logistic probability function is then fitted to the data series of D and the function is then standardised following the classical approximation of Abramowitz and Stegun (1965). SPEI also ranges between -2 and +2, the average value of the SPEI is 0, and the standard deviation is 1 (Vicente-Serrano et al., 2010a; Vicente-Serrano et al., 2010b).

3.2.2 Agricultural drought indicators

Agricultural droughts are defined as the lack of soil moisture to fulfil crop demands, and therefore the agriculture sector is normally the first to be affected by a drought. In this study we characterize agricultural droughts by means of two spatially distributed indicators defined as follows:

Evapotranspiration Deficit Index (ETDI)

The ETDI (Narasimhan and Srinivasan, 2005) is computed from the anomaly of water stress to its long term average. The monthly water stress ratio (WS [0-1]) is computed as:

$$WS = \frac{PET - AET}{PET} \quad (1)$$

where PET and AET are the monthly reference potential evaporation and monthly actual evaporation, respectively. The monthly water stress anomaly (WSA) is calculated as:

$$WSA_{y,m} = \frac{MWS_m - WS_{y,m}}{MWS_m - \min WS_m} \times 100, \text{ if } WS_{y,m} \leq MWS_m \quad (2)$$

$$WSA_{y,m} = \frac{MWS_m - WS_{y,m}}{\max WS_m - MWS_m} \times 100, \text{ if } WS_{y,m} > MWS_m \quad (3)$$

where MWS_m is the long-term median of water stress of month m , $\max MWS_m$ is the long-term maximum water stress of month m , $\min WS_m$ is the long-term minimum water stress of month m , and WS is the monthly water stress ratio ($y = 1979-2010$ and $m = 1-12$). Narasimhan and Srinivasan (2005) scaled the ETDI between -4 and 4 to be comparable with PDSI. Here we used the same scaling procedure but amended this to scale ETDI between -2 and 2 to make it comparable to SPI, SPEI and SRI:

$$ETDI_{y,m} = 0.5ETDI_{y,m-1} + \frac{WSA_{y,m}}{100} \quad (4)$$

Root Stress Anomaly Index (RSAI)

The ‘root stress’ (RS) is a spatial indicator of the available soil moisture, or the lack of it, in the root zone. The root stress varies from 0 to 1, where 0 indicates that the soil water availability in the root zone is at field capacity and 1 indicates that the soil water availability in the root zone is zero and the plant is under maximum water stress. The RSAI is computed similarly to the ETDI described above. The monthly root stress anomaly (RSA) is calculated as:

$$RSA_{y,m} = \frac{MRS_m - RS_{y,m}}{MRS_m - \min RS_m} \times 100, \text{ if } RS_{y,m} \leq MRS_m \quad (5)$$

$$RSA_{y,m} = \frac{MRS_m - RS_{y,m}}{\max RS_m - MRS_m} \times 100, \text{ if } RS_{y,m} > MRS_m \quad (6)$$

where MRS_m is the long-term median root stress of month m , $maxMRS_m$ is the long-term maximum root stress of month m , $minRS_m$ is the long-term minimum root stress of month m , and $RS_{y,m}$ is the monthly root stress ($y= 1979-2010$ and $m= 1-12$). The root stress anomaly index, scaled between -2 and 2 (using the same procedure as Narasimhan and Srinivasan, 2005) is:

$$RSAI_{y,m} = 0.5RSAI_{y,m-1} + \frac{RSA_{y,m}}{100} \quad (7)$$

3.2.3 Hydrological drought indicators

For the characterisation of hydrological droughts we used the commonly applied Standardized Runoff Index (SRI, Shukla and Wood, 2008) for streamflow and Groundwater Resource Index (GRI, Mendicino et al., 2008) for groundwater storage.

Standardized Runoff Index (SRI)

SRI follows the same concept as SPI and is defined as a "unit standard normal deviate associated with the percentile of hydrologic runoff accumulated over a specific duration" (Shukla and Wood, 2008). To compute SRI the simulated runoff time series is fitted to a probability density function (a gamma distribution is used here) and the function is used to estimate the cumulative probability of the runoff of interest for a specific month and temporal scale. The cumulative probability is then transformed to the standardised normal distribution with mean zero and variance one (Shukla and Wood, 2008).

Groundwater Resource Index (GRI)

$GRI_{y,m}$ is suggested as a standarisation of the monthly values of groundwater storage (detention) without any tranformation (Mendicino et al., 2008):

$$GRI_{y,m} = \frac{S_{y,m} - \mu_{S,m}}{\sigma_{S,m}} \quad (8)$$

where $S_{y,m}$ is the value of the groundwater storage for the year y and the month m , and $\mu_{S,m}$ and $\sigma_{S,m}$ are respectively the mean and the standard deviation of the groundwater storage S simulated for the month m in a defined number of years (32 years in this case). The same classification that is used for the SPI (between -2 and +2) is applied to GRI (Wanders et al., 2010).

3.3 Identification of past droughts and primary characterization of drought severity

To identify past droughts, the drought indicators described were calculated for the period 1979-2010 for the Limpopo river basin, resulting in times series of monthly indicator maps. The maps allow for the visualization of the spatial variability of the indicators in the basin. SPI, SPEI and SRI were computed for different aggregation periods (1, 3, 6, 12, and 24). All the indicators were then aggregated over several sub-basins resulting in times series for each indicator. The historical sub-

basin-averaged indicators were then compared. Maps of the indicators are also compared for specific years to show the spatial variability of the indicators and the extent of the droughts.

All indices considered were scaled to range between -2 and 2. Based on the SPI values, droughts may be classified into mild ($0 > \text{SPI} > -1$), moderate ($-1 \geq \text{SPI} > -1.5$), severe ($-1.5 \geq \text{SPI} > -2$) and extreme ($\text{SPI} \leq -2$) (Lloyd-Hughes and Saunders, 2002, see Table 3). For SPI and SPEI the spatially averaged indicators are not anymore related with a probability of occurrence. However, we still use the same thresholds for the characterization of the sub-basin aggregated droughts, as we understand that the resulting indicators would not be very different from the computation of these indicators with aggregated precipitation and potential evaporation. For agricultural (ETDI and RSAI) and groundwater indicators (GRI) this is not the case as these are not defined based on a probability of occurrence.

Droughts are generally characterized by a start date and an end date (both defining duration), drought intensity (Indicator value), and severity or drought magnitude. The drought severity (DS) definition by McKee et al. (1993) is used here:

$$DS = -(\sum_{j=1}^x Iv_{ij}) \quad (9)$$

Where Iv is the indicator value, j starts with the first month of a drought and continues to increase until the end of the drought (x) for any of the i time scales. The DS [months] would be numerically equivalent to the drought duration if each month the drought had an intensity (value) of -1.0 (McKee et al., 1993).

4 Results and discussion

4.1 Hydrological model performance

Given the complexity of the basin for hydrological modelling, particularly due to the arid/semi-arid nature, the model results are quite satisfactory, especially for the larger sub-basins. Runoff estimates from the hydrological model were verified with observed runoff on a monthly basis. For a number of the runoff stations tested, the coefficient of determination (R^2) values varied from about 0.45 to as good as 0.92. In a review on model application and evaluation, Moriasi et al. (2007) recommended three quantitative statistics for model evaluation: Nash-Sutcliffe efficiency (NSE), percent bias (PBIAS), and the ratio of the root mean square error to the standard deviation of the measured data (RSR). They also specified ranges for these statistics for a "satisfactory" model performance (NSE > 0.5, RSR \leq 0.70, and PBIAS \pm 25% for steamflow). However, PBIAS is highly influenced by uncertainty in the observed data (Moriasi et al., 2007). Given the potential problems in observed flow data in South Africa reported by the Water Research Commission (2009) such as poor accuracy of the rating table, particularly at low flows and the inability to measure high flows, we do not evaluate our

results based on PBIAS. The evaluation measures NSE and RSR together with the coefficient of determination for selected stations are presented in Table 4. We do not calibrate parameters based on these evaluation measures, but we use them as a simple test of concordance. Based on the ranges proposed by Moriasi et al. (2007), the model performance is found to be satisfactory for four out of six runoff stations.

4.2 Identification of historic hydrological droughts in the basin

Drought indicators were computed for the period 1979-2010. Agricultural and hydrological drought indicators were computed from the fluxes resulting from the hydrological model. Because the focus in the current model is to simulate hydrological droughts, it is important that the model captures the most important drought events in the simulation period 1979-2010. DEWFORA (2012) reported that in the period 1980-2000, the Southern African region was struck by four major droughts, notably in the seasons 1982/83, 1986/87, 1991/92 and 1994/95. The drought of 1991/92 was the most severe in the region in recent history. After the year 2000, important droughts include the years 2002/03/04 and 2005/06. Droughts in the Limpopo river basin also show significant spatial variability. A study covering only the Botswana part of the basin documents a severe drought that occurred in 1984 (Dube and Sekhwela, 2007). However, in that year no documentation of drought in the other parts of the basin was found.

4.2.1 Agricultural droughts

Figure 2 presents RSAI and ETDI for the most severe drought in the recent history (1991/92), for the very dry year 1982/83, for a wet year (1999/2000), and for a year with both dry and wet conditions at different locations in the basin (1984/85), respectively. The geographic variability of the RSAI seems to be slightly higher than that of ETDI. These indicators provide information for the assessment of agricultural droughts. The figure shows that both indicators, computed from different outputs of the hydrological model (actual evaporation and soil moisture), produce similar results and are able to reproduce the dry/wet conditions in the basin. This is also supported by Fig. 3, which shows the fraction of the Limpopo basin under moderate to extreme agricultural drought, i.e. $I_v < -1.0$. Both indicators illustrate that a large part of the basin was under at least moderate agricultural drought conditions for the years with recorded droughts events.

4.2.2 Hydrological droughts

Figure 4 shows the SRI values (1-month, 3-months, 6-months, and 12-months) from 1979 to 2010 computed from the simulated runoff at station #24. The dotted grey line at the threshold value of -1 is used to identify moderate droughts, with the moderate drought considered to start when the indicator downcrosses the threshold, and stop when the indicator upcrosses the threshold. The simulated SRI clearly identifies the severe hydrological droughts of 1982/83 and 1991/92, and the very wet (flood)

year of 1999/2000. SRI from observed data was not included in the figure given that there are periods with missing data and the computation of SRI requires a monthly runoff data set for a continuous period without missing data.

The Groundwater Resource Index (GRI) presented in Fig. 5 for the same selected years shows the years 1991/92 and 1982/83 to be drier than normal but the intensity of the drought appears to be quite low (not severe). The year 1984/85, selected as it presents both dry and wet conditions at different locations in the basin, does not show this spatial variability for GRI. This could be expected due to the persistence of the groundwater storage and low intensity of indicators of drought/wetness in this year in different locations of the basin. The intensity of the extremely wet year 1999/2000 is well represented, suggesting that GRI is skewed. This is likely due to the fact that GRI is not transformed into the normal space. Moreover, the distribution of values is constrained by the capacity of the groundwater reservoir in the hydrological model. Mendicino et al. (2008) applied this indicator in a Mediterranean climate but the skewness test of normality showed that their series from January to September were normally distributed, while the series of October to December were not normally distributed. However, they indicate that the values of groundwater storage in the last winter months and in spring were more important. For this indicator to be applied independently of the climate and basin conditions it should probably be transformed into the normal space.

4.2.3 Comparison of drought indicators

The computed indicators were averaged for the whole basin as well as for the selected sub-basins. Time series of the resulting indicators were compared for the whole 1979-2010 period. Figure 6 presents the time series of aggregated drought indicators for sub-basin #24. Note that the sub-basins are named after the hydrometric station number. Figure 6 compares the agricultural, hydrological and groundwater drought indicators. The agricultural indicators ETDI and RSAI are compared with the meteorological drought indicators SPI and SPEI with a short aggregation period (3 months) that are commonly used as indicators of agricultural droughts. Figure 6 upper plot shows that the indices are mostly in phase, correctly representing the occurrence of dry and wet years, and the intensities of the events are in general quite similar. The hydrological drought indicator SRI-6 is compared with the meteorological drought indicators SPI-6 and SPEI-6 (upper middle plot). All three indicators roughly follow the same pattern, but the fluctuation of the SRI seems to be slightly lower than that of the meteorological indices (SPI and SPEI). This is probably due to the higher persistence of streamflow when compared to precipitation. Moreover, it is clearly visible from Fig. 6 that the temporal variability or fluctuation of the indicators reduces when moving from drought indicators associated to agricultural to those associated to hydrological drought. This means that several mild agricultural droughts do not progress further to hydrological droughts. Moreover, to identify groundwater droughts, or major

drought events, the time series of GRI is compared to the time series of meteorological drought indicators with long aggregation periods (SPI-12, SPEI-12, SRI-12, SPI-24, SPEI-24, SRI-24) (see Fig. 6, lower middle and lower plots). The plots show that as the variability of the indicator reduces further the number of multi-year prolonged droughts increases. However, for groundwater droughts only two events (1982/83 and 1991/92) are identified as moderate to severe droughts ($I_v < -1$). The plots again show that in general the temporal variability of the runoff-derived indicator (SRI) is lower than that of the meteorological indicators (SPI and SPEI). The GRI index shows much less temporal variability than the other indices and does not identify any extreme events with the exception of the flood of 1999/2000. Similar results using GRI were found by Wanders et al (2010), who indicate that GRI has a very low number of droughts with a high average duration. Moreover, a study of Peters and Van Lanen (2003) investigated groundwater droughts for two climatically contrasting regimes. For the semi-arid regime they found multi-annual droughts to occur frequently. They indicate that the effect of the groundwater system is to pool erratically occurring dry months into prolonged groundwater droughts for the semi-arid climate.

Table 5 presents a correlation matrix between all the indicators considered in this study for sub-basin #24. Similar correlation results were found for the other sub-basins. The table shows that the agricultural drought indicators ETDI and RSAI have the highest correlation with SPEI-3, SPEI-6, SPI-3, SPI-6 and with SRI with low aggregation periods (1 to 3 months). For every station the correlation between the agricultural indicators and SPEI is slightly higher than with SPI. While the hydrological drought indicators SRI-6 and SRI-12 present the highest correlation with the meteorological drought indicators SPI-12 and SPEI-12, the extended hydrological drought indicator SRI-24 is better correlated with the meteorological drought indicators SPI-24 and SPEI-24. GRI shows the highest correlation with SRI-6 and SRI-12. This makes sense given the direct connection between groundwater and runoff, where groundwater (baseflow) contributes to the total runoff.

Figure 7, Fig. 8 and Fig. 9 present the monthly spatial mean time series of drought indicators for sub-basins #1, 18 and 20, respectively. The averaged indicators for sub-basins #24 and 1, the two largest sub-basins considered, are almost identical (see Fig. 6 and Fig. 7). Figure 8 shows that even though the general pattern of the time series for the sub-basin #18 is similar to that found for sub-basin # 24 and 1, some differences are noticeable. For example, Fig. 8 shows a clear drought period for sub-basin #18 in the years 1984/85/86 which is not apparent for the sub-basins #24 and 1. These localised drought events that affected the upper part of the basin were not apparent for the lower part of the basin. This was also observed in Fig. 2. Moreover, the extreme floods that occurred in the lower part of the basin in 1999/2000 are much less severe in the upstream parts of the basin. For example, Fig. 9 shows that for sub-basin #20 (the smallest sub-basin considered), the flood of 1996/97 was more severe than that of 1999/2000. Similarly, while the drought of 2003/04 is quite mild when averaged over the largest

selected sub-basin (#24), it is quite severe for sub-basin #20 (similar to the droughts of 1983/84 and 1991/92).

For the four sub-basins a short but intense agricultural drought is noticeable at the beginning of the 2005/06 season, but this did not progress to be an extended hydrological drought. This is coherent with the literature, which indicates that this season was delayed, and after a dry start of the season, good rainfall occurred from the second half of December (Department of Agriculture of South Africa, 2006). In sub-basin #18 (Fig. 8) even though meteorological indicators (SPI-6, SPEI-6, SPI-12, and SPEI-12) suggest that the 1986/87 season was near normal to wet, the hydrological indicators (SRI-6, SRI-12) point to a dry runoff year. Measured runoff at this station indicates that indeed the year 1986/87 was a dry year. This seems similar to what was found by Peters and van Lanen (2003), for the longer aggregations periods an accumulation of successive short anomalies can lead to an overall hydrological drought. Similarly, meteorological indicators suggest that the floods of 1996/97 and 1999/2000 in the lower part of the basin were of similar magnitude. However, records indicate that the flood of 1999/2000 was much more extreme than the one of 1996/97 (WMO, 2012). This can be clearly seen in the hydrological drought indicators SRI-6, SRI-12, SRI-24. GRI index shows almost no departure from normal with the exception of the flood of 1999/2000. These results show the importance of computing indicators that can be related to hydrological drought, and how these add value to the identification of droughts/floods and their severity. The indicators also help identify the spatial and temporal evolution of drought and flood events that would otherwise not have been apparent when considering only meteorological indicators.

We also computed drought severities (DS [months]) resulting from the different indicators as explained in section 3.3 (Eq. 9). The droughts of 1982/83, 1986/87, 1991/92, 1994/95, 2002/03/04, and 2005/06 are identified among the most severe droughts, but the ending month of these drought events varies for the different indicators. The indicators with higher aggregation periods (e.g 12 and 24 months), which have a lower temporal variability, generally point to longer droughts (multi-year droughts) with higher persistence than indicators with lower aggregation periods (agricultural droughts). For example, while the agricultural indicators suggest that the extreme drought of 1991/92 is over by the end of 1992 or beginning of 1993, the indicators that represent hydrological droughts point out that this drought only ends at the end of 1993. Moreover, for SRI-12, GRI, SPI-24 and SPEI-24 this multi-year drought lasts until 1994/95. As an example for sub-basin #24, Fig. 10 presents the duration and severity of the six most severe recorded droughts as identified by the meteorological drought indicator SPEI aggregated for different periods to represent agricultural, hydrological and extended hydrological droughts (multi-year droughts). The graph shows that the multi-year droughts resulting from the accumulation of shorter successive droughts are the most severe as a result of the duration. These droughts can be the most hazardous, as a succession of mild droughts that can initially seem non-problematic can result in very severe droughts if they last for a long time. The average

intensity of these droughts is generally lower than that of the agricultural droughts, which can be very intense but often of shorter duration.

5 Conclusions

Very low runoff coefficients and high rainfall variability pose major challenges in modelling hydrological droughts in (semi-)arid basins. Small errors in the meteorological forcing and estimation of evaporation may result in significant errors in the runoff estimation. This also implies that model calibration, if any, should be applied cautiously to maintain the physical meaning of model parameters. We opted to apply a process-based model and parameterize it on the basis of the best available input data without additional calibration. In the process we ensured that we were using reliable datasets and interpolated or aggregated them with care to prepare spatially distributed parameter maps. The model is able to simulate hydrological drought related indices reasonably well. We have derived a number of different drought indicators from the model results, such as ETDI, RSAI, SRI, and GRI. While the SRI is based on river runoff at a particular river section, the ETDI, RSAI and GRI are spatial indicators that can be estimated at any location in the basin. ETDI and RSAI are directly related to water availability for vegetation with or without irrigation, and GRI is related with the groundwater storage. Moreover, we computed the widely known drought indicators SPI and SPEI at different aggregation periods to verify the correlation of the different aggregation periods for these indicators and the different types of droughts.

All the indicators considered (with the exception of GRI) are able to represent the most severe droughts in the basin and to identify the spatial variability of the droughts. Our results show that even though meteorological indicators with different aggregation periods serve to characterise droughts reasonably well, there is added value in computing indicators based on the hydrological model for the identification of droughts/floods and their severity. The indicators also help identify the spatial and temporal evolution of drought and flood events that would otherwise not have been apparent when considering only meteorological indicators.

RSAI follows greatly ETDI, and ETDI is quite well represented by SPEI-3 and SPEI-6. This indicates that in the absence of actual evaporation and soil moisture data which are required to compute ETDI and RSAI, the meteorological indicator SPEI-3 which considers both precipitation and potential evaporation and is reasonably easy to compute may be used as an indicator of agricultural droughts. For discharge we observe some added value in computing SRI. Even though SPI can give a reasonable indication of droughts conditions, computing SRI can be more effective for the identification of hydrological droughts. The groundwater indicator GRI mostly remains near normal conditions. A combination of different indicators, such as SPEI-3, SRI-6, and SPI-12 (computed together), can be an effective way to characterise from agricultural to long-term hydrological droughts in the Limpopo river basin.

1 **Acknowledgements**

2 This study was carried out in the scope of the DEWFORA (Improved Drought Early Warning and
3 Forecasting to strengthen preparedness and adaptation to droughts in Africa) project which is funded
4 by the Seventh Framework Programme for Research and Technological Development (FP7) of the
5 European Union (Grant agreement no: 265454).

6

References

- Abramowitz, M., and Stegun, I. A.: Handbook of mathematical functions, with formulas, graphs, and mathematical tables, Dover Publications, 1046 pp., 1965.
- Allen, R. G., Pereira, L., Raes, D., and Smith, M.: Crop evapotranspiration - Guidelines for computing crop water requirements: FAO Irrigation and drainage paper No. 56, FAO, Rome, 26-40, 1998.
- Alley, W. M.: The Palmer Drought Severity Index: Limitations and Assumptions, Journal of Climate and Applied Meteorology, 23, 1100-1109, doi: 10.1175/1520-0450(1984)023<1100:tpdsil>2.0.co;2, 1984.
- Alston, M., and Kent, J.: Social impacts of drought, Centre for Rural Social Research, Charles Sturt University, Wagga Wagga, NSW, 2004.
- Balsamo, G., Boussetta, S., Lopez, P., and Ferranti, L.: Evaluation of ERA-Interim and ERA-Interim-GPCP-rescaled precipitation over the USA, ECMWF ERA Report Series 5, 1-25, available at: <http://www.ecmwf.int/publications/library/do/references/list/782009>, last access: December 2013, 2010.
- Barbosa, P., Naumann, G., Valentini, L., Vogt, J., Dutra, E., Magni, D., and De Jager, A.: A Pan-African map viewer for drought monitoring and forecasting, 14th Waternet Symposium, Dar es Salaam, Tanzania, 30 October to 1 November 2013,
- Dee, D. P., Uppala, S. M., Simmons, A. J., Berrisford, P., Poli, P., Kobayashi, S., Andrae, U., Balmaseda, M. A., Balsamo, G., Bauer, P., Bechtold, P., Beljaars, A. C. M., van de Berg, L., Bidlot, J., Bormann, N., Delsol, C., Dragani, R., Fuentes, M., Geer, A. J., Haimberger, L., Healy, S. B., Hersbach, H., Hólm, E. V., Isaksen, L., Kållberg, P., Köhler, M., Matricardi, M., McNally, A. P., Monge-Sanz, B. M., Morcrette, J. J., Park, B. K., Peubey, C., de Rosnay, P., Tavalato, C., Thépaut, J. N., and Vitart, F.: The ERA-Interim reanalysis: configuration and performance of the data assimilation system, Quarterly Journal of the Royal Meteorological Society, 137, 553-597, doi: 10.1002/qj.828, 2011.
- Department of Agriculture of South Africa: Crops and markets - First quarter 2006, Vol 87., No. 927, Directorate Agricultural Statistics - Department of Agriculture http://www.daff.gov.za/docs/statsinfo/Crops_0106.pdf, last access: December 2013, 2006.
- DEWFORA: WP6-D6.1 - Implementation of improved methodologies in comparative case studies - Inception report for each case study, DEWFORA Project - EU FP7, www.dewfora.net, last access: December 2013, 2012.

- 1 Dube, O. P., and Sekhwela, M. B. M.: Community coping strategies in Semiarid Limpopo basin part
2 of Botswana: Enhancing adaptation capacity to climate change,
3 http://www.aiaccproject.org/working_papers/Working%20Papers/AIACC_WP47_Dube.pdf, last
4 access: December, 2013, 1-40, 2007.
- 5 Dürre, H. H., Meybeck, M., and Dürre, S. H.: Lithologic composition of the Earth's continental surfaces
6 derived from a new digital map emphasizing riverine material transfer, *Global Biogeochemical*
7 *Cycles*, 19, GB4S10, doi: 10.1029/2005GB002515, 2005.
- 8 FAO: Irrigation Potential in Africa: A Basin Approach, FAO-UN, Rome, 1997.
- 9 FAO, The digital soil map of the world (Version 3.6), FAO-UN, Rome:
10 <http://www.fao.org/geonetwork/srv/en/metadata.show?id=14116&currTab=distribution>, access: 21
11 August 2012, 2003.
- 12 Glantz, M. H. e.: Drought and Hunger in Africa: Denying Famine a Future, Cambridge University
13 Press, Cambridge, 1987.
- 14 Guttman, N. B.: Comparing the Palmer Drought Index and the Standardized Precipitation Index,
15 *JAWRA Journal of the American Water Resources Association*, 34, 113-121, doi: 10.1111/j.1752-
16 1688.1998.tb05964.x, 1998.
- 17 Hagemann, S., Botzet, M., Dümenil, L., and Machein, B.: Derivation of global GCM boundary
18 conditions from 1 km land use satellite data, MPI Report No. 289, Max Planck Institute for
19 Meteorology, Hamburg, 1999.
- 20 Hagemann, S.: An improved land surface parameter dataset for global and regional climate models,
21 MPI Report No. 336, Max Planck Institute for Meteorology, Hamburg, 2002.
- 22 Hargreaves, G. H., and Allen, R. G.: History and Evaluation of Hargreaves Evapotranspiration
23 Equation, *Journal of Irrigation and Drainage Engineering*, 129, 53-63, 2003.
- 24 Huffman, G. J., Adler, R. F., Bolvin, D. T., and Gu, G.: Improving the global precipitation record:
25 GPCP version 2.1, *Geophys. Res. Lett.*, 36, L17808, doi:10.1029/2009GL040000, 2009.
- 26 IPCC: Climate Change 2007: The Physical Science Basis. Contribution of Working Group I to the
27 Fourth Assessment, Report of the Intergovernmental Panel on Climate Change [Solomon, S., D. Qin,
28 M. Manning, Z. Chen, M. Marquis, K.B. Averyt, M. Tignor and H.L. Miller (eds.)], Cambridge
29 University Press, Cambridge, United Kingdom and New York, NY, USA, 996 pp., 2007.
- 30 Keyantash, J., and Dracup, J. A.: The quantification of drought: an evaluation of drought indices,
31 *Bulletin of the American Meteorological Society*, 83, 1167-1180, 2002.

- 1 LBPTC: Joint Limpopo River Basin Study Scoping Phase. Final Report. BIGCON Consortium.,
2 Limpopo Basin Permanent Technical Committee,
3 http://www.limcom.org/_system/writable/DMSStorage/1031en/LIMCOM2010_ScopingStudy_Eng.pdf,
4 last access: December 2013, 2010.
- 5 Lehner, B., Döll, P., Alcamo, J., Henrichs, T., and Kaspar, F.: Estimating the impact of global change
6 on flood and drought risks in Europe: a continental, integrated analysis, *Climatic Change*, 75, 273-299,
7 2006.
- 8 Lloyd-Hughes, B., and Saunders, M. A.: A drought climatology for Europe, *International Journal of*
9 *Climatology*, 22, 1571-1592, doi: 10.1002/joc.846, 2002.
- 10 McKee, T. B., Doesken, N. J., and Kleist, J.: The relationship of drought frequency and duration to
11 time scales, *Proceedings of the 8th Conference on Applied Climatology*, Vol. 17. No. 22, Boston, MA:
12 American Meteorological Society, 17, 179-183, 1993.
- 13 Mendicino, G., Senatore, A., and Versace, P.: A Groundwater Resource Index (GRI) for drought
14 monitoring and forecasting in a mediterranean climate, *Journal of Hydrology*, 357, 282-302, doi:
15 <http://dx.doi.org/10.1016/j.jhydrol.2008.05.005>, 2008.
- 16 Moriasi, D., Arnold, J., Van Liew, M., Bingner, R., Harmel, R., and Veith, T.: Model evaluation
17 guidelines for systematic quantification of accuracy in watershed simulations, *Transactions of the*
18 *ASABE*, 50, 885-900, 2007.
- 19 Narasimhan, B., and Srinivasan, R.: Development and evaluation of Soil Moisture Deficit Index
20 (SMDI) and Evapotranspiration Deficit Index (ETDI) for agricultural drought monitoring, *Agricultural*
21 *and Forest Meteorology*, 133, 69-88, doi: <http://dx.doi.org/10.1016/j.agrformet.2005.07.012>, 2005.
- 22 Palmer, W. C.: Meteorological drought, Research paper no.45, US Department of Commerce, Weather
23 Bureau Washington, DC, USA, 1-58, 1965.
- 24 Patz, J. A., Campbell-Lendrum, D., Holloway, T., and Foley, J. A.: Impact of regional climate change
25 on human health, *Nature*, 438, 310-317, 2005.
- 26 Peters, E., and Van Lanen, H. A. J.: Propagation of drought in groundwater in semiarid and sub-humid
27 climatic regimes, in: *Hydrology in Mediterranean and semiarid regions: International conference*,
28 Montpellier, France, 2003, 312–317, IAHS Press, Wallingford, UK, 2003.
- 29 Pilgrim, D. H., Chapman, T. G., and Goran, D. G.: Problems of rainfall-runoff modelling in arid and
30 semiarid regions, *Hydrological Sciences Journal*, 33:4, 379-400, doi: 10.1080/02626668809491261,
31 1988.

1 Schulze, R. E.: Hydrological simulation as a tool for agricultural drought assessment, *Water S. A.*, 10,
2 55-62, 1984.

3 Sheffield, J., and Wood, E. F.: Projected changes in drought occurrence under future global warming
4 from multi-model, multi-scenario, IPCC AR4 simulations, *Climate Dynamics*, 31, 79-105, 2008.

5 Shukla, S., and Wood, A. W.: Use of a standardized runoff index for characterizing hydrologic
6 drought, *Geophysical research letters*, 35, L02405, doi: 10.1029/2007gl032487, 2008.

7 Siebert, S., Döll, P., Feick, S., Hoogeveen, J., and Frenken, K.: Global Map of Irrigation Areas
8 version 4.0.1, ed: Johann Wolfgang Goethe University, Frankfurt am Main, Germany / Food and
9 Agriculture Organization of the United Nations, Rome, Italy, 2007.

10 Szczypta, C., Calvet, J. C., Albergel, C., Balsamo, G., Boussetta, S., Carrer, D., Lafont, S., and
11 Meurey, C.: Verification of the new ECMWF ERA-Interim reanalysis over France, *Hydrology and*
12 *Earth System Sciences*, 15, 647-666, 2011.

13 Trambauer, P., Maskey, S., Winsemius, H., Werner, M., and Uhlenbrook, S.: A review of continental
14 scale hydrological models and their suitability for drought forecasting in (sub-Saharan) Africa, *Physics*
15 *and Chemistry of the Earth*, 66, 16-26, doi: <http://dx.doi.org/10.1016/j.pce.2013.07.003>, 2013.

16 Trambauer, P., Dutra, E., Maskey, S., Werner, M., Pappenberger, F., van Beek, L. P. H., and
17 Uhlenbrook, S.: Comparison of different evaporation estimates over the African continent, *Hydrol.*
18 *Earth Syst. Sci.*, 18, 193-212, 10.5194/hess-18-193-2014, 2014.

19 USGS EROS, Africa Land Cover Characteristics Data Base Version 2.0:
20 http://edc2.usgs.gov/glcc/tablamert_af.php, access: 24 June 2012, 2002.

21 USGS EROS, Hydro1K Africa
22 http://eros.usgs.gov/#/Find_Data/Products_and_Data_Available/gtopo30/hydro/africa, access: 21
23 September 2012, 2006.

24 van Beek, L. P. H.: Forcing PCR-GLOBWB with CRU data, Utrecht University, Utrecht, Netherlands:
25 <http://vanbeek.geo.uu.nl/suppinfo/vanbeek2008.pdf>, last access: December 2013, 2008.

26 van Beek, L. P. H., and Bierkens, M. F. P.: The Global Hydrological Model PCR-GLOBWB:
27 Conceptualization, Parameterization and Verification, Utrecht University, Faculty of Earth Sciences,
28 Department of Physical Geography, Utrecht, The Netherlands, 2009.

29 van Beek, L. P. H., Wada, Y., and Bierkens, M. F. P.: Global monthly water stress: 1. Water balance
30 and water availability, *Water Resour. Res.*, 47, W07517, doi: 10.1029/2010WR009791, 2011.

- 1 Vicente-Serrano, S. M., Beguería, S., and López-Moreno, J. I.: A Multiscalar Drought Index Sensitive
2 to Global Warming: The Standardized Precipitation Evapotranspiration Index, *Journal of Climate*, 23,
3 1696-1718, doi: 10.1175/2009jcli2909.1, 2010a.
- 4 Vicente-Serrano, S. M., Beguería, S., López-Moreno, J. I., Angulo, M., and El Kenawy, A.: A New
5 Global 0.5° Gridded Dataset (1901–2006) of a Multiscalar Drought Index: Comparison with Current
6 Drought Index Datasets Based on the Palmer Drought Severity Index, *Journal of Hydrometeorology*,
7 11, 1033-1043, 2010b.
- 8 Wanders, N., Lanen, H. A. J., and van Loon, A. F.: Indicators for Drought Characterization on a
9 Global Scale. WATCH Water and Global change EU FP6. Technical report No. 24, [http://www.eu-](http://www.eu-watch.org/publications/technical-reports/3)
10 [watch.org/publications/technical-reports/3](http://www.eu-watch.org/publications/technical-reports/3), last access: December 2013, 2010.
- 11 Water Research Commission: IWR Rhodes University, School of BEEH University of KwaZulu-
12 Natal, and Water for Africa: Identification, estimation, quantification and incorporation of risk and
13 uncertainty in water resources management tools in South Africa. Deliverable No. 3: Interim Report
14 on Sources of Uncertainty, Water Research Commission Project No: K5/1838 2009.
- 15 WMO: Limpopo River basin - A proposal to improve the flood forecasting and early warning system,
16 World Meteorological Organization,
17 http://www.wmo.int/pages/prog/hwrrp/chy/chy14/documents/ms/Limpopo_Report.pdf, last access:
18 December 2013, 2012.
- 19 Zhu, T., and Ringler, C.: Climate Change Impacts on Water Availability and Use in the Limpopo
20 River Basin, *Water*, 4, 63-84, 2012.

1

Table 1 Drought indicators derived in this study

Name	Variable	Type of drought	Purpose/Reason	Reference
SPI	Precipitation	Meteorological	Particularly important for rainfed agriculture as well as influences farming practises	McKee et al., 1993
SPEI	Precipitation/ Evaporation	Meteorological	As SPI, but with a more detailed focus on available water	Vicente-Serrano et al., 2010b
ETDI (Evapotranspiration deficit index)	Evaporation	Agricultural	Impact on yield as a result of water availability for evaporation	Narasimhan and Srinivasan, 2005
RSI (Root stress anomaly index)	Root stress	Agricultural	Impacts on root growth and yield	This study
SRI (Standardized runoff index)	Discharge	Hydrological	River discharge is important for many aspects such as shipping, irrigation, energy	Shukla and Wood, 2008
GRI (Groundwater resource index)	Groundwater	Hydrological	Groundwater is used for irrigation and drinking water	Mendicino et al., 2008

2

3

Table 2 Naturalized and observed runoff coefficients for selected stations

Station number	Sub-basin area (km ²)	Number of years without missing data	Mean annual observed runoff (m ³ /s)	RCnat	RCobs
24	342,000	27	96.9	4.3	1.7
23	259,436	26	82.1	3.8	2.0
1	201,001	17	39.5	3.0	1.2
18	98,240	29	12.2	3.6	0.7
20	12,286	24	14.8	6.3	5.3
15	7,483	32	4.6	6.3	3.1

4

5

Table 3 State definition according to the Index value

Index value (Iv)	State category
$Iv \geq 2.0$	Extremely wet
$1.5 \leq Iv < 2.0$	Severely wet
$1.0 \leq Iv < 1.5$	Moderately wet
$0 \leq Iv < 1.0$	Mildly wet
$-1.0 \leq Iv < 0$	Mild drought
$-1.5 \leq Iv < -1.0$	Moderate drought
$-2.0 \leq Iv < -1.5$	Severe drought
$Iv < -2.0$	Extreme drought

6

Table 4 Model evaluation measures for runoff for selected stations

Station number	R ²	NSE	RSR
24	0.92	0.90	0.32
23	0.62	0.38	0.79
1	0.69	0.57	0.65
18	0.68	0.62	0.62
20	0.70	0.65	0.59
15	0.53	0.48	0.72

Table 5 correlation matrix for sub-basin 24

	SPI-3	SPEI-3	ETDI	RSAI	SPI-6	SPEI-6	SRI-1	SRI-2	SRI-3	SRI-6	SPI-12	SPEI-12	SRI-12	SPI-24	SPEI-24	SRI-24	GRI
SPI-3	1.00																
SPEI-3	0.91	1.00															
ETDI	0.79	0.82	1.00														
RSAI	0.70	0.73	0.84	1.00													
SPI-6	0.77	0.75	0.81	0.79	1.00												
SPEI-6	0.72	0.80	0.83	0.80	0.94	1.00											
SRI-1	0.69	0.71	0.84	0.84	0.74	0.75	1.00										
SRI-2	0.67	0.71	0.83	0.85	0.75	0.78	0.97	1.00									
SRI-3	0.63	0.68	0.81	0.85	0.75	0.78	0.94	0.99	1.00								
SRI-6	0.51	0.58	0.75	0.82	0.71	0.76	0.87	0.93	0.96	1.00							
SPI-12	0.53	0.56	0.70	0.74	0.73	0.75	0.72	0.75	0.78	0.82	1.00						
SPEI-12	0.48	0.58	0.68	0.71	0.68	0.77	0.69	0.73	0.75	0.81	0.96	1.00					
SRI-12	0.37	0.45	0.61	0.65	0.53	0.61	0.74	0.80	0.83	0.91	0.81	0.83	1.00				
SPI-24	0.45	0.48	0.56	0.59	0.60	0.63	0.65	0.68	0.69	0.72	0.79	0.80	0.76	1.00			
SPEI-24	0.40	0.48	0.52	0.54	0.54	0.62	0.60	0.62	0.64	0.67	0.71	0.79	0.73	0.96	1.00		
SRI-24	0.30	0.35	0.44	0.46	0.42	0.47	0.60	0.64	0.67	0.71	0.57	0.62	0.80	0.83	0.84	1.00	
GRI	0.37	0.34	0.48	0.57	0.48	0.42	0.72	0.75	0.76	0.76	0.57	0.48	0.73	0.60	0.49	0.66	1.00

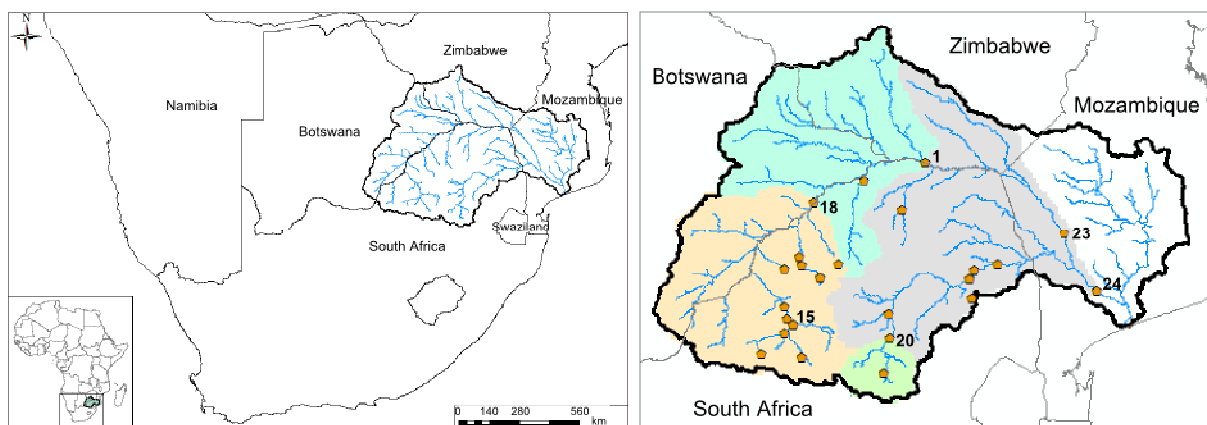


Fig. 1 Limpopo river basin: the location of the basin (left) and the locations of hydrometric stations (right). Selected stations (#1, 15, 18, 20, 23, and 24) are highlighted. The sub-basins draining to each hydrometric station are named after the station number.

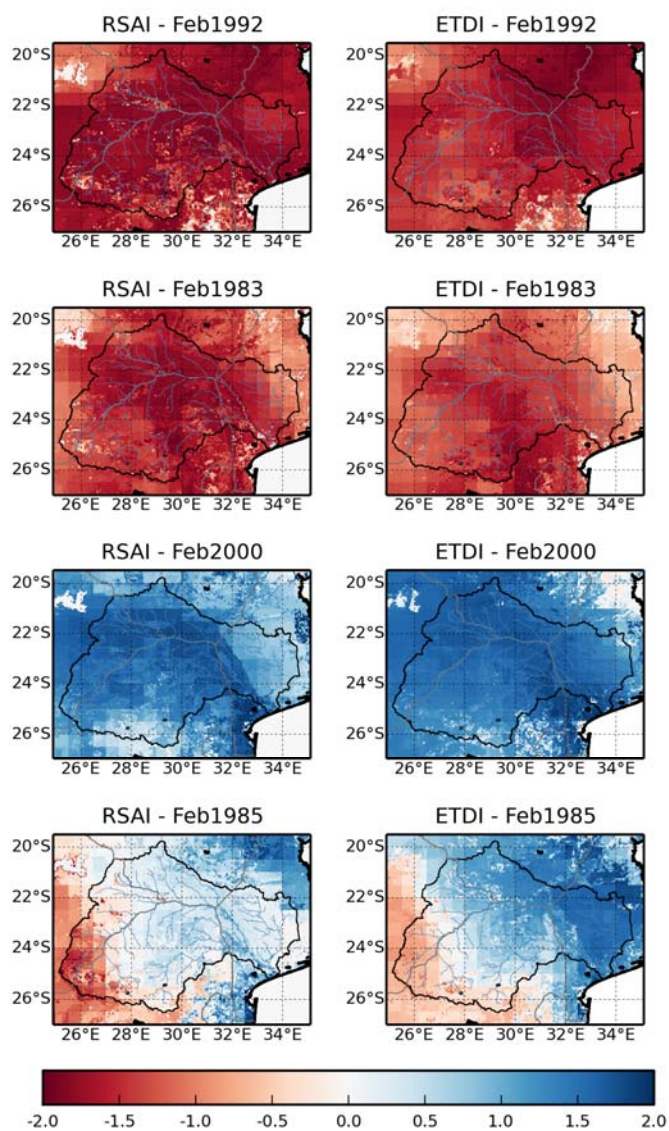


Fig. 2 Root stress anomaly index (RSAI) and Evapotranspiration Deficit Index (ETDI) in the Limpopo basin for selected years

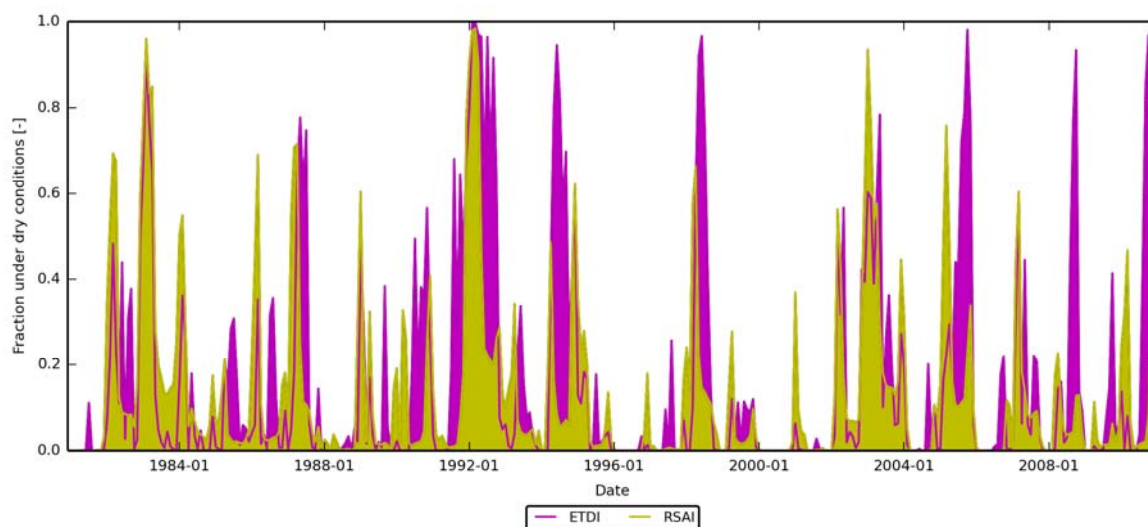


Fig. 3 Fraction of the Limpopo basin under moderate to extreme droughts represented by the indicator value ($I_v < -1.0$)

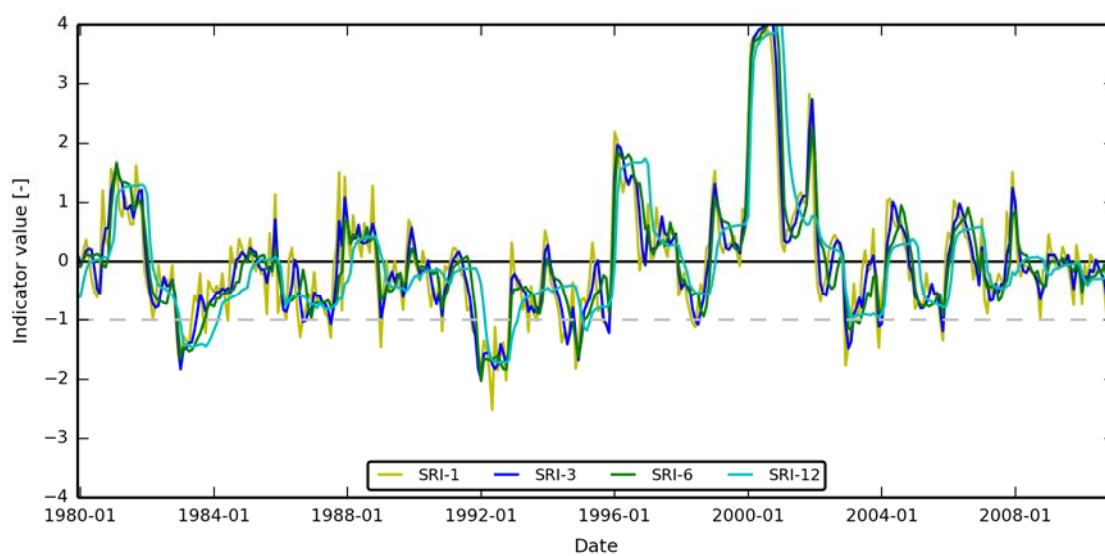
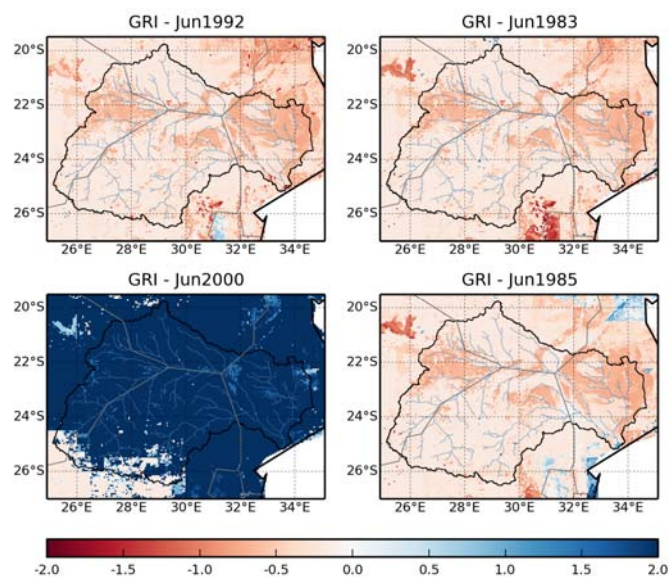


Fig. 4 Simulated SRI for station #24



1

2 Fig. 5 Groundwater resource Index (GRI) for selected years

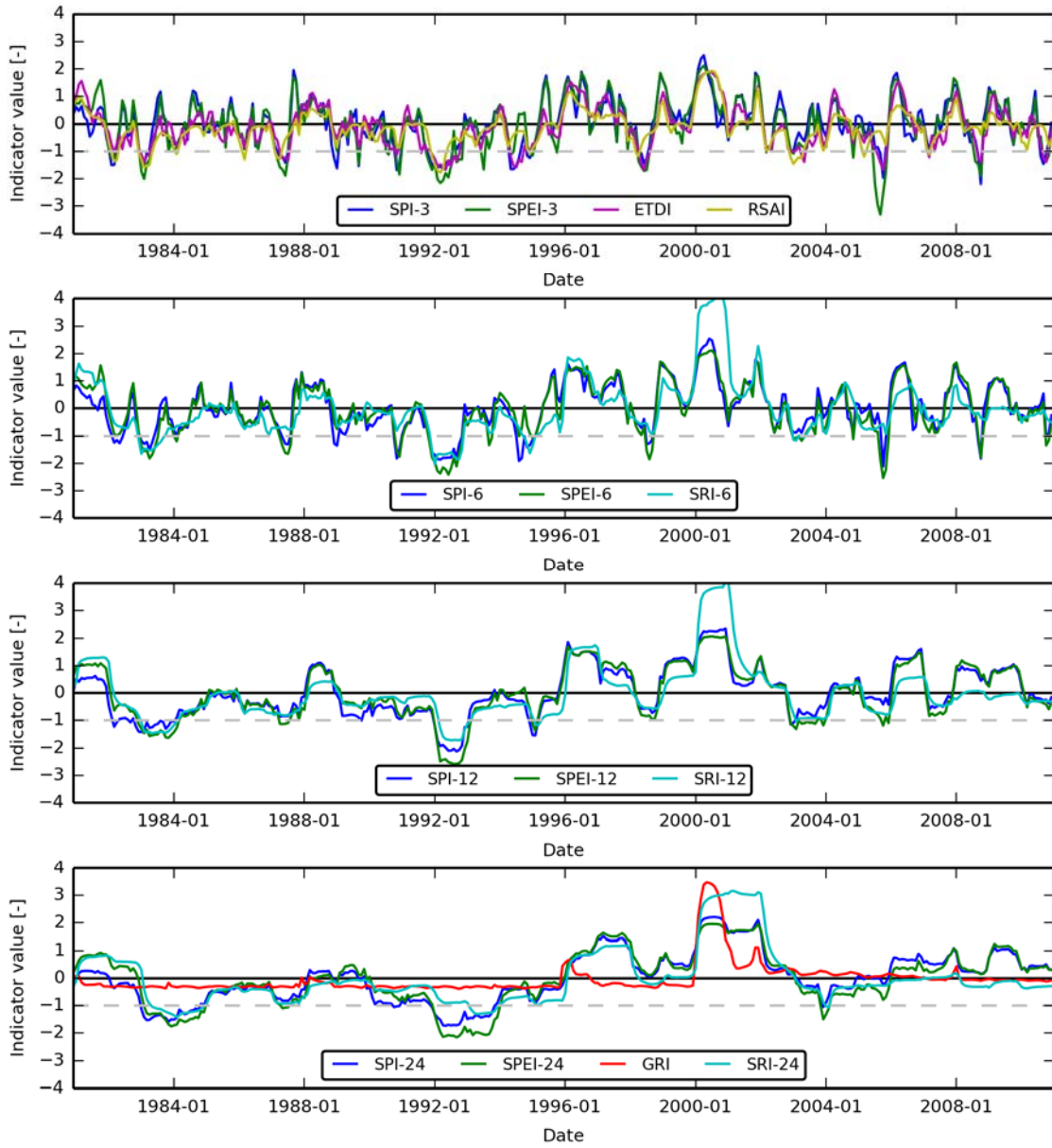
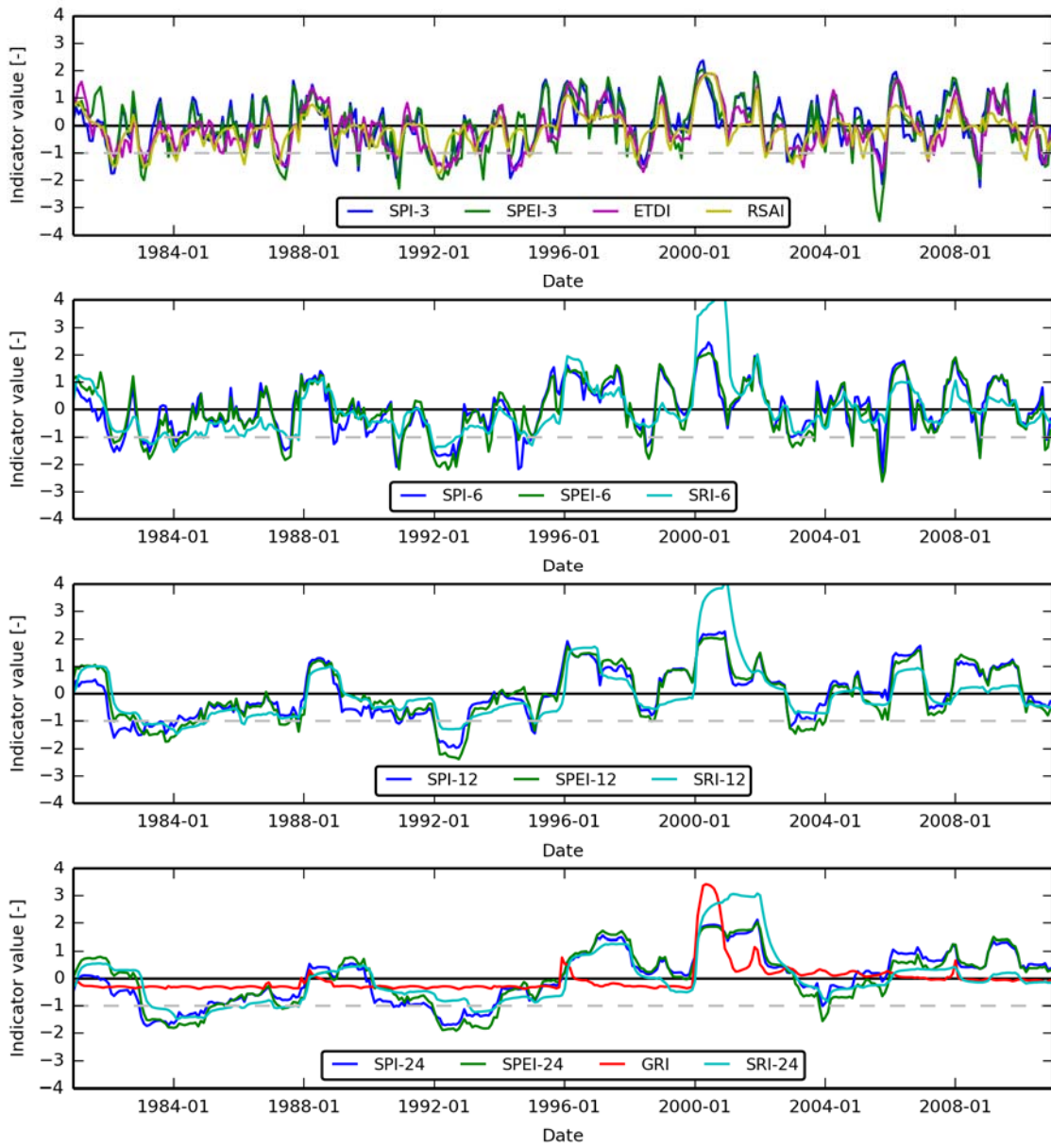
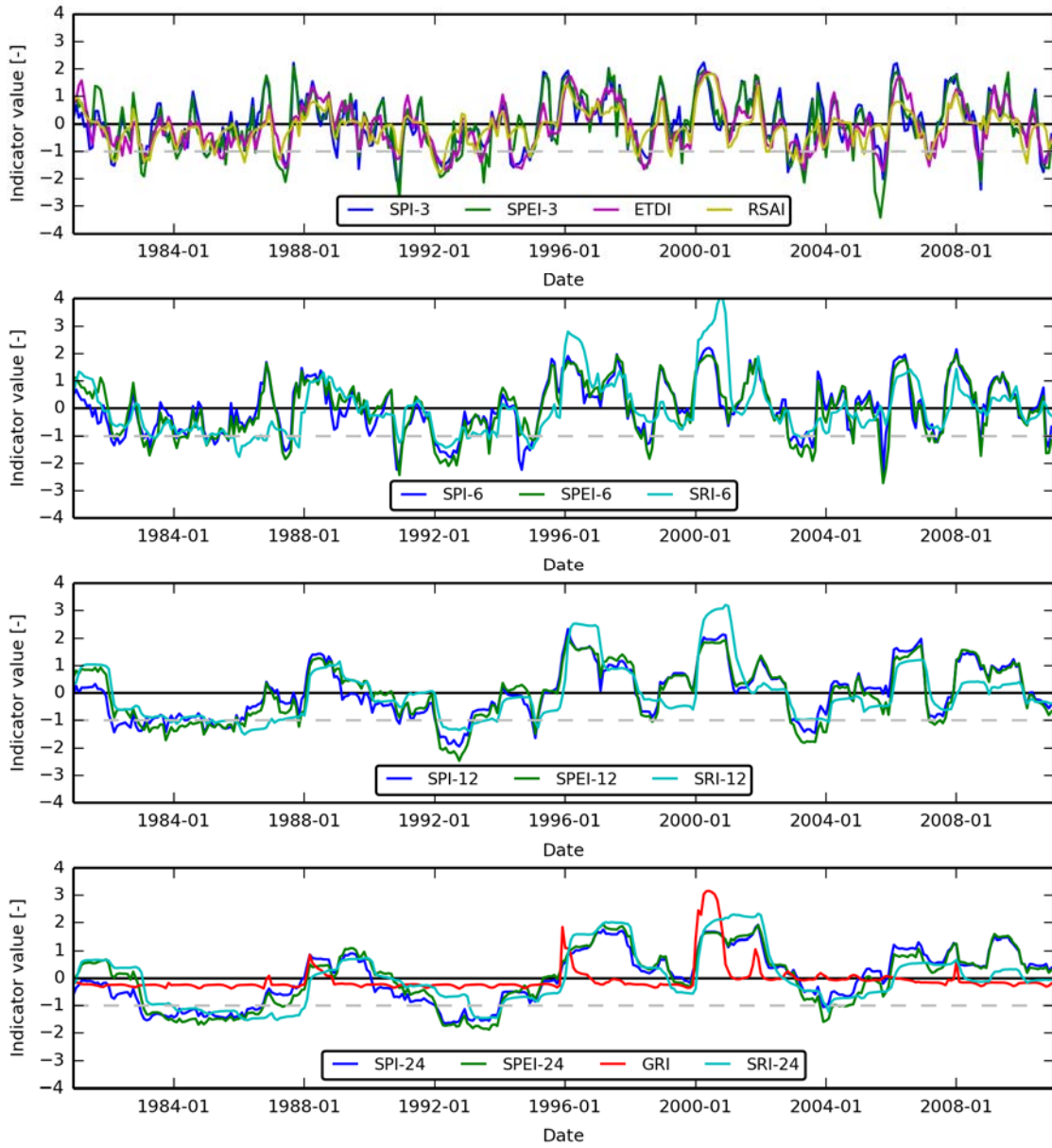


Fig. 6 Time series of aggregated drought indicators for sub-basin #24. Upper graph: Indicators used to characterize agricultural droughts (SPI-3, SPEI-3, ETDI, and RSAI), upper middle graph: indicators used to characterize hydrological drought (SPI-6, SPEI-6, and SRI-6), lower middle graph: indicators used to characterize groundwater droughts (SPI-12, SPEI-12, and SRI-12), and lower graph: indicators used to characterize extended groundwater droughts (SPI-24, SPEI-24, GRI, and SRI-24).



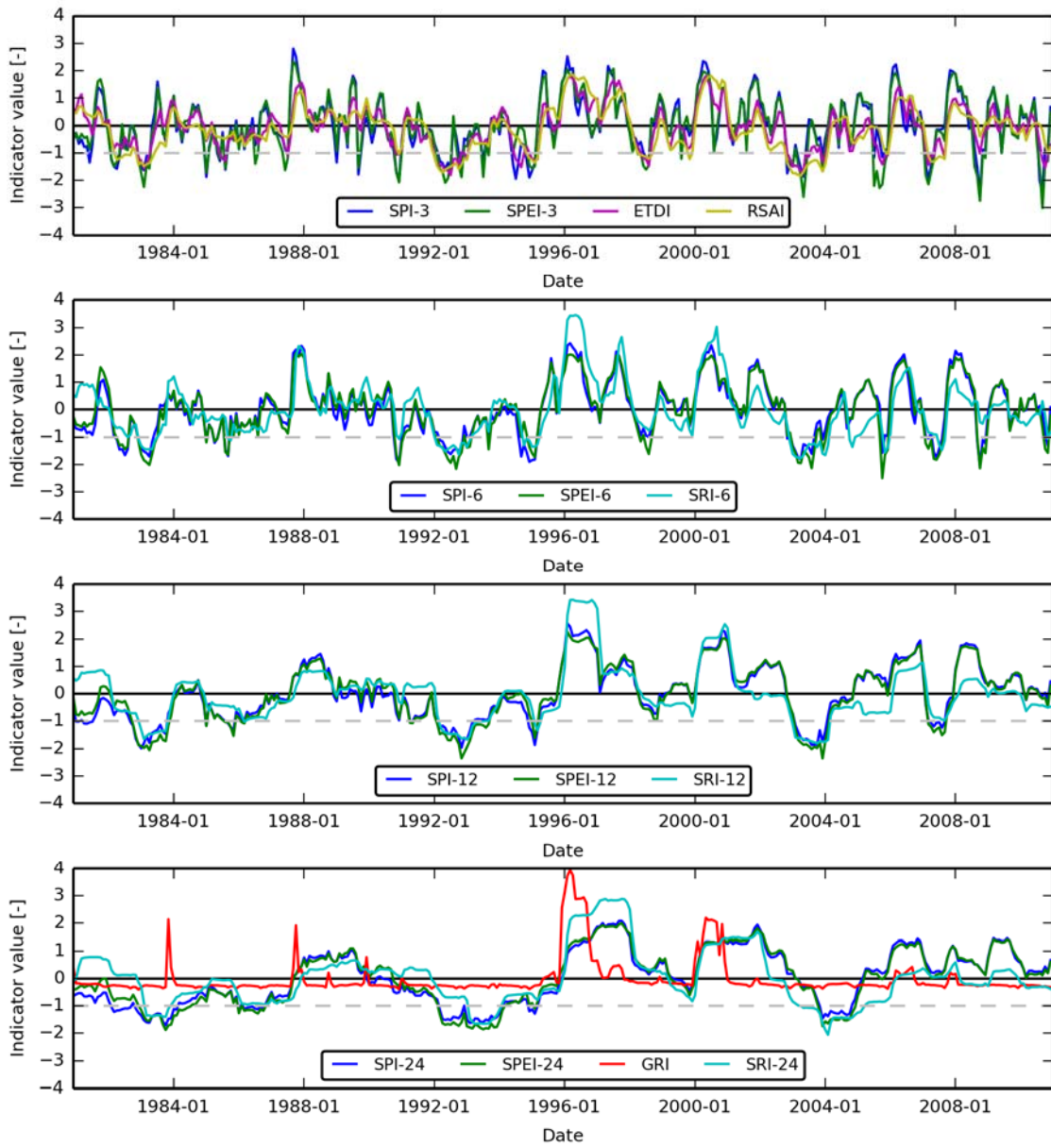
1

2 Fig. 7 Same as Fig. 5 for sub-basin #1.



1

2 Fig. 8 Same as Fig. 5 for sub-basin #18.



1

2 Fig. 9 Same as Fig. 5 for sub-basin #20.

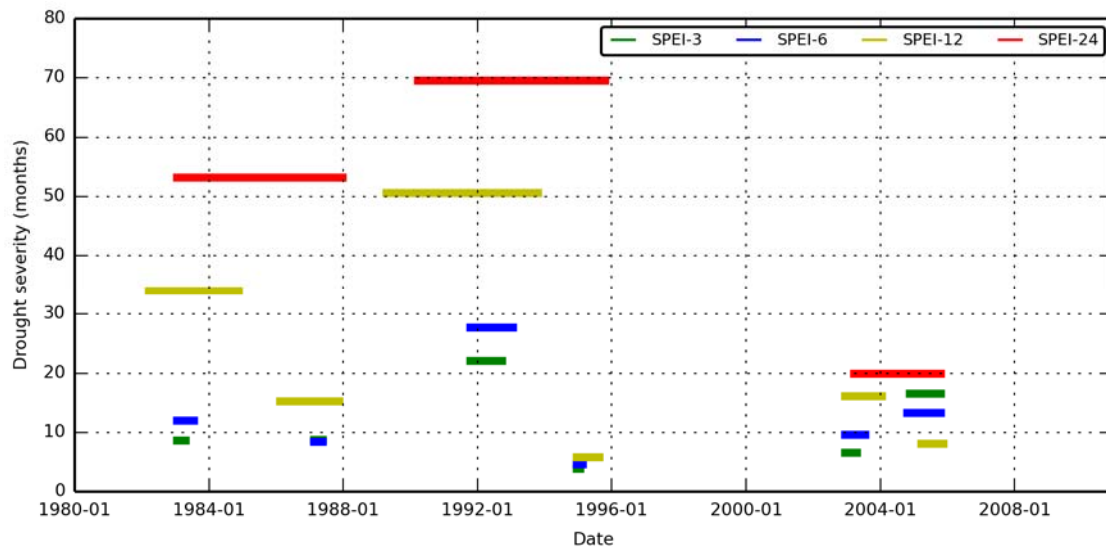


Fig. 10 Drought severity and duration in sub-basin #24 for the 6 most severe droughts in the period 1979-2010 for the indicator SPEI with different aggregation periods.